

Combined Solution of the Inverse Stefan Problem for Successive Freezing/Thawing in Nonideal Biological Tissues

Y. Rabin¹

A. Shitzer

Department of Mechanical Engineering,
Technion—Israel Institute of Technology,
Haifa, Israel 32000

A new combined solution of the one-dimensional inverse Stefan problem in biological tissues is presented. The tissue is assumed to be a nonideal material in which phase transition occurs over a temperature range. The solution includes the thermal effects of blood perfusion and metabolic heat generation. The analysis combines a heat balance integral solution in the frozen region and a numerical enthalpy-based solution approach in the unfrozen region. The subregion of phase transition is included in the unfrozen region. Thermal effects of blood perfusion and metabolic heat generation are assumed to be temperature dependent and present in the unfrozen region only. An arbitrary initial condition is assumed that renders the solution useful for cryosurgical applications employing repeated freezing/thawing cycles. Very good agreement is obtained between the combined and an exact solution of a similar problem with constant thermophysical properties and a uniform initial condition. The solution indicated that blood perfusion does not appreciably affect either the shape of the temperature forcing function on the cryoprobe or the location and depth of penetration of the freezing front in peripheral tissues. It does, however, have a major influence on the freezing/thawing cycle duration, which is most pronounced during the thawing stage. The cooling rate imposed at the freezing front also has a major inverse effect on the duration of the freezing/thawing.

Introduction

One of the critical factors in determining the success of a cryosurgical procedure relates to the control of the cooling rate during phase change (Mazur, 1963; Orpwood, 1981; Fahy, 1981). It is customary to assume that at very low or, alternatively, at very high cooling rates maximum tissue destruction is achieved (Farrant, 1971; Miller and Mazur, 1976; Akhtar et al., 1979; Gage et al., 1985; Augustynowicz and Gage, 1985). These cooling rates are of the order of a few, or hundreds of degrees Centigrade per minute, at the two extremes of the spectrum, respectively (Rubinsky and Onik, 1991).

The thawing rate applied to the tissue at the end of the freezing process also affects the outcome of the cryosurgical procedure. Thus, slow thawing rates may enhance cell destruction (Miller and Mazur, 1976). Uncontrolled thawing, due to natural heat exchange with surrounding tissues and the environment, may be deemed sufficiently slow for this application. Other experiments demonstrated that under certain circumstances, high thawing rates may be conducive to tissue destruction, e.g., red blood cells (Akhtar et al., 1979). Additional evidence indicates that the extent of damage caused by cryosurgery may be appreciably enhanced by the application of successive cooling/thawing cycles to the tissue (Gage et al., 1985; Rand et al., 1985).

Ordinary heat transfer problems involving change of phase, in which the boundary conditions are specified at the external, stationary surface, are usually referred to as "Stefan problems" (Stefan, 1891). Those problems for which the boundary conditions are specified at the moving phase-change front are usually

termed "inverse Stefan problems". In this group of problems, the temperature forcing function at the stationary boundary is one of the sought-after results. The requirement of certain cooling rates at the moving boundary in biological tissues undergoing cryosurgery classifies them as inverse Stefan problems.

Change of phase in biological tissues, which are highly nonideal substances in the thermal sense, occurs over a rather wide temperature range. The upper limit of this range may be between -0.5°C to -1°C , while the lower limit may be between -5°C to -8°C (Altman and Dittmer, 1971; Wessling and Blackshear, 1973). This wide range of temperatures excludes the direct application of existing analytical solutions to inverse Stefan problems. This is because these solutions were developed for problems involving pure materials in which phase change occurs at a single, well-defined temperature (Carslaw and Jaeger, 1959; Rubinsky and Shitzer, 1976). The only existing analytical solution that addresses phase change problems in biological tissues was developed for a uniform initial temperature in the tissue (Rabin and Shitzer, 1995). It thus does not permit the consideration of successive multiple freezing/thawing cycles. Moreover, the analyses presented by Rubinsky and Shitzer (1976) and Rabin and Shitzer (1995) assume constant blood perfusion and metabolic heat generation rates, which are known to be temperature dependent. The only approximate analytical solution (Budman et al., 1995) that treats the biological tissue as nonideal substances subjected to arbitrary initial conditions, disregards the thermal effects of either blood perfusion or metabolic heat generation.

In this article a combined solution to the one-dimensional, inverse Stefan problem in biological tissues is presented in Cartesian coordinates. The solution combines an approximate analytical approach in the frozen region with a numerical analysis of the unfrozen region. In both regions the solutions are based on integral methods. In the frozen region the thermophysical properties are constant and the temperature distribution is

¹ Present address: Department of Mechanical Engineering, Carnegie Mellon University, Pittsburgh, PA 15213.

Contributed by the Bioengineering Division for publication in the JOURNAL OF BIOMECHANICAL ENGINEERING. Manuscript received by the Bioengineering Division November 15, 1994; revised manuscript received June 30, 1996. Associate Technical Editor: K. R. Diller.

derived from energy conservation considerations in the entire region (Goodman, 1958; Voller, 1986). In the unfrozen region the solution is calculated numerically according to a temperature-dependent specific heat, which is defined using the enthalpy approach (also known as the "weak solution"; Shamsundar and Sparrow, 1975). The biological tissue is treated as a nonideal substance in which change of phase occurs over a given temperature range. The solution incorporates the thermal effects of blood perfusion and metabolic heat generation, both of which are assumed to be temperature dependent in the unfrozen region. The solution is developed for any given arbitrary initial temperature distribution.

The combined solution is rather general in nature and can be applied to solving nonbiological problems as well. This is done by simply setting the terms representing blood perfusion and metabolic heat generation to zero. Examples to the wide class of problems that can thus be analyzed are the determination of optimal cooling rates in the frozen food industry, prevention of thermal stresses in metal solidification, etc.

Problem Definition

For the purpose of the combined solution, let the fully frozen region be defined by the index f and the rest of the medium by index u . This implies that both the unfrozen and the phase transition regions, are grouped into a single subregion in the analysis. As a consequence, a single freezing front, s , is defined that represents the lower limit of the temperature range over which phase change occurs, T_{mf} . This front actually separates the fully frozen region from the rest of the medium. It, thus, also separates the region in which the approximate analytical solution is applied from that which is analyzed numerically.

The following additional assumptions are made:

- The problem is one dimensional and semi-infinite.
- The thermal conductivity is a steplike function across the freezing front, possessing two constant, but different values, Fig. 1.
- The volumetric specific heat is temperature dependent in the unfrozen region, u , and possesses a constant value in the frozen region, f , Fig. 1. In the phase transition subregion, this property is taken as an effective one, which includes the latent heat of phase change (Goodman, 1958).
- Metabolic heat generation is temperature dependent in the unfrozen region, and is absent in the frozen region, Fig. 1.
- Blood perfusion is temperature dependent in the unfrozen region, and is absent in the frozen region, Fig. 1.
- Blood temperature is constant in time and uniform in the arteries supplying the tissue. This assumption is particularly applicable in peripheral tissues.

Nomenclature

C = volumetric specific heat, $\text{J/m}^3\text{-}^\circ\text{C}$
 H = cooling rate, $^\circ\text{C/s}$
 k = thermal conductivity, $\text{W/m-}^\circ\text{C}$
 n = node number
 \dot{q}_{met} = metabolic heat generation rate, W/m^3
 \bar{q} = metabolic heat generation parameter, Eq. (7), $^\circ\text{C/s}$
 s = phase-change interface location, m
 \dot{s} = phase-change interface velocity, m/s
 t = time, s
 T = temperature, $^\circ\text{C}$
 \dot{w}_b = volumetric blood perfusion rate, 1/s

\tilde{w} = blood perfusion parameter, Eq. (6), 1/s
 x = coordinate, m
 α = thermal diffusivity, m^2/s
 β = nondimensional interface velocity in the numerical solution, Eq. (13)
 γ = nondimensional blood perfusion in the numerical solution, Eq. (14)
 λ = nondimensional thermal diffusivity in the numerical solution, Eq. (12)
 μ = nondimensional metabolic heat generation in the numerical solution, Eq. (15)
 ξ = transformed coordinate, Eq. (5), m
 φ = constant in the temperature distribution in the frozen region, 1/m

ψ = total enthalpy per unit area of the frozen region, Eq. (20), J/m^2

Subscripts

0 = initial
 b = blood
 f = frozen
 i = nodes counter
 met = metabolic
 ml = upper limit of phase transition temperature range
 mf = lower limit of phase transition temperature range
 p = time counter
 u = unfrozen

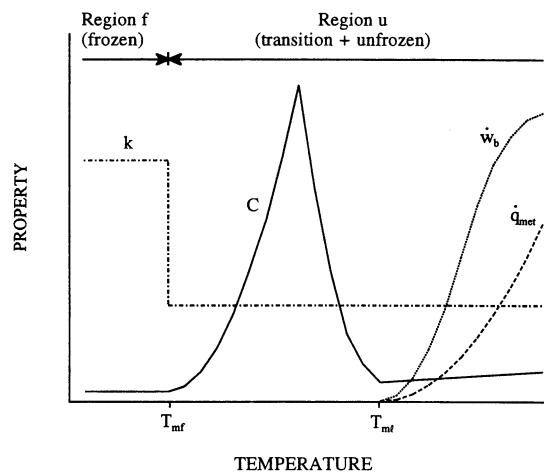


Fig. 1 Schematic representation of the assumed temperature dependence of thermal and thermophysiological properties

- The initial temperature is a known arbitrary function.

Figure 1 represents the schematic behavior of the various properties listed above. However, the functional behavior of these properties needs to be defined for computational purposes. The properties are assumed to be dependent on temperature as follows: Metabolic heat generation rate is represented by the Q10 exponential function (Eberhart, 1985). Blood perfusion is assumed to vary linearly from a constant value at normal tissue temperature down to zero at the upper temperature limit of phase transition. Volumetric specific heat is composed of two linear segments, which intersect at the peak temperature of the phase transition region. The slopes of the linear segments are chosen such that the integral of the specific heat over the phase transition temperature range equals the sum of the latent plus sensible heats (Comini and del Giudice, 1976; Rabin and Shitzer, 1995). Outside the phase-change region the volumetric specific heat is assumed to be constant at different values. Values used in this study are listed in Table 1.

Analysis

It is customary to assume that in those biological tissues characterized by relatively low blood perfusion rates and a dense distribution of capillary vessels, e.g., peripheral tissues, the heat balance in the unfrozen region is given by the bio-heat equation (Pennes, 1948):

Table 1 Typical thermophysiological properties of biological tissues in peripheral areas

| | |
|---|----------------------------|
| Uniform initial temperature | 37 °C |
| Blood temperature | 37 °C |
| Upper phase change temperature | -1 °C |
| Peak phase change temperature | -3 °C |
| Lower phase change temperature | -8 °C |
| Thermal conductivity in the unfrozen region | 0.5 W/m·°C |
| Thermal conductivity in the frozen region | 2.0 W/m·°C |
| Volumetric specific heat in the unfrozen region | 3.6 MJ/m ³ ·°C |
| Volumetric specific heat in the frozen region | 1.8 MJ/m ³ ·°C |
| Latent heat of freezing | 233.4 MJ/m ³ |
| Volumetric specific heat source of the blood | 0.25 kW/m ³ ·°C |

$$C_u \frac{\partial T}{\partial t} = k_u \frac{\partial^2 T}{\partial x^2} + \dot{w}_b C_b (T_b - T) + \dot{q}_{met} \quad s \leq x < \infty \quad (1)$$

When the interface location, s , is known, the heat transfer process in this region is well defined mathematically by specifying temperature boundary conditions at the freezing front and at infinity, respectively:

$$T(s, t) = T_{mf} \quad (2a)$$

$$T(\infty, t) = T_\infty \quad (2b)$$

and by defining an initial condition:

$$T(x, 0) = T_0(x) \quad s \leq x \leq \infty \quad (2c)$$

It is, thus, possible to obtain a mathematical solution for the temperature distribution in the unfrozen region independent of the temperature distribution in the adjacent frozen region.

The location of the freezing front may be determined by applying Stefan's condition of a constant cooling rate at this front:

$$\left. \frac{\partial T}{\partial t} \right|_+ (s, t) = H_u \quad (3)$$

where the "+" sign indicates the unfrozen region.

An additional condition is necessary to specify the initial location of the freezing front. In the present analysis, freezing occurs over a range of temperatures. Thus, two distinct fronts may be identified: the temperature front, T_{ml} , at which the first ice crystals begin to form and the second, T_{mf} , behind which the freezing process is fully completed. This second front is defined here as the "freezing front." The simplest case, insofar as the initial location of this freezing front is concerned, is the one for which no fully frozen regions exist initially in the medium. This condition is expressed mathematically by:

$$s(0) = 0 \quad (4)$$

For a general initial condition and temperature-dependent thermophysical properties, the temperature distribution and

the location of the freezing front may be calculated by numerical techniques only. The numerical solution is developed in a coordinate system, the origin of which tracks the freezing front:

$$\xi = x - s \quad (5)$$

For convenience, additional parameters are defined by:

$$\tilde{w} \equiv \frac{\dot{w}_b C_b}{C_u} \quad (6)$$

$$\tilde{q} \equiv \frac{\dot{q}_{met}}{C_u} \quad (7)$$

$$T(\xi, t) \equiv T(x, t) - T_b \quad (8)$$

Application of Eqs. (5) – (8) transforms the governing equation and boundary and initial conditions to:

$$\frac{\partial T}{\partial t} = \alpha_u \frac{\partial^2 T}{\partial \xi^2} + s \frac{\partial T}{\partial \xi} - \tilde{w}T + \tilde{q}_u \quad 0 \leq \xi \leq \infty \quad (9)$$

$$T(0, t) = T_{mf} - T_b \quad (10a)$$

$$T(\infty, t) = T_\infty - T_b \quad (10b)$$

$$T(\xi, 0) = T_0(x) - T_b \quad (10c)$$

where in Eq. (10c) it is tacitly assumed that initially there does not exist a frozen region immediately adjacent to the interface with the cryoprobe. It is noted that the proposed solution does not exclude the existence of frozen regions inside the medium away from the outer interface. However, in cryosurgical applications, and for obtaining maximal tissue destruction, the thawing of the frozen tissue should be complete before the next freezing cycle is initiated.

In the transformed coordinate system ξ , Stefan's condition of a constant cooling rate on the freezing front is expressed by:

$$-s \left. \frac{\partial T}{\partial \xi} \right|_+ (0, t) = H_u \quad (11)$$

It follows from this condition that at a quasi-steady state, wherein the temperature gradient on the freezing front is constant in time, the requirement of a constant cooling rate thereon will impose a constant velocity of the freezing front. For this condition the present analysis coincides with a previous exact solution to the problem (Rabin and Shitzer, 1995).

Numerical solution of Eq. (9) in the unfrozen region may be obtained by a modified Crank–Nicholson technique (Carnahan et al., 1969). For the purposes of the present analysis this technique should be adapted to include the thermal effects of metabolic heat generation and blood perfusion. The numerical solution is performed in terms of the following dimensionless variables:

$$\lambda_i^{p-1/2} \equiv \frac{\alpha_i^{p-1/2} \Delta t}{2(\Delta \xi)^2} \quad (12)$$

$$\beta_i^{p-1/2} \equiv \frac{s \Delta t}{4(\Delta \xi)} \quad (13)$$

$$\gamma_i^{p-1/2} \equiv \frac{1}{2} \tilde{w}_i^{p-1/2} \Delta t \quad (14)$$

$$\mu_i^{p-1/2} \equiv \tilde{q}_i^{p-1/2} \Delta t \quad (15)$$

The bio-heat equation, Eq. (9), is rewritten next in terms of these variables:

$$\begin{aligned}
 & -(\lambda_i^{p-1/2} - \beta_i^{p-1/2})T_{i-1}^p \\
 & + (1 + 2\lambda_i^{p-1/2} + \gamma_i^{p-1/2})T_i^p - (\lambda_i^{p-1/2} + \beta_i^{p-1/2})T_{i+1}^p \\
 & = (\lambda_i^{p-1/2} - \beta_i^{p-1/2})T_{i-1}^{p-1} + (1 - 2\lambda_i^{p-1/2} - \gamma_i^{p-1/2})T_i^{p-1} \\
 & + (\lambda_i^{p-1/2} + \beta_i^{p-1/2})T_{i+1}^{p-1} + \mu_i^{p-1/2} \quad (16)
 \end{aligned}$$

Temperature distribution in the unfrozen region is obtained by simultaneously solving Eq. (16) for all the numerical grid points. The $n \times n$ coefficient matrix may be made to be tridiagonal, by careful selection of the grid points, which is then easily solvable by Thomas' algorithm. Since in this problem the thermophysical properties are strongly temperature dependent, particularly during phase change, a solution by the predictor-corrector method is suggested as follows:

(a) Estimation of the temperature distribution at time level p by the thermophysical properties and temperature distribution at time level $p - 1$;

(b) Assessment of the values of the thermophysical properties at time level $p - \frac{1}{2}$ by the average temperature distributions at time levels $p - 1$ and p ; and,

(c) Recalculation of the temperature distribution at time level p by the values of the thermophysical properties at time level $p - \frac{1}{2}$ and the temperature distribution at time level $p - 1$. The resulting numerical scheme is of a second order both in time and in space and converges unconditionally (Carnahan et al., 1969).

We now turn to analyzing the frozen region. In this region the bio-heat equation, Eq. (1), reduces to a simple heat balance equation due to the absence of blood perfusion and metabolic activities. Assuming constant and uniform thermophysical properties, this equation is given by:

$$C_f \frac{\partial T}{\partial t} = k_f \frac{\partial^2 T}{\partial x^2} \quad 0 \leq x \leq s \quad (17)$$

subjected to boundary conditions presenting continuity requirements in the temperature and in the heat flux at the freezing front:

$$T(s, t) = T_{mf} \quad (18a)$$

$$-k_f \frac{\partial T}{\partial x} \Big|_{(s, t)}^- = -k_u \frac{\partial T}{\partial x} \Big|_{(s, t)}^+ \quad (18b)$$

Note that a free boundary condition is tacitly assumed on the cryoprobe surface. It was assumed that no fully frozen region exists initially in the medium, Eq. (4). Thus:

$$T(x \rightarrow 0, t = 0) = T_{mf} \quad (18c)$$

The solution of the frozen region is performed by an integral method (Goodman, 1958; Voller, 1986). The functional behavior of the temperature distribution is assumed first. The coefficients of this function are calculated next, using the integral form of Eq. (17), yielding:

$$T = T_{mf} - \frac{k_u H_u}{\varphi k_f s} \{1 - \exp[\varphi(s - x)]\} \quad (19)$$

which satisfies both the boundary and initial conditions, Eqs. (18a)–(18c). To calculate the coefficient φ in Eq. (19), the total enthalpy, ψ , of the frozen region is defined by:

$$\psi \equiv \int_0^s C_f (T - T_{mf}) dx \quad (20)$$

The change in this property during each time interval, conforming to the numerical solution of the unfrozen region, may

be calculated in two ways. One is through the requirement that the heat balance equation, Eq. (17), be satisfied in the integral sense. The second is by substitution of the assumed temperature distribution in the frozen region, Eq. (19), into Eq. (20). Equating the results obtained by these operations would yield the value of the coefficient φ .

First, Eq. (17) is integrated across the entire frozen region, $0 \leq x \leq s$, to yield:

$$\int_0^s C_f \frac{\partial T}{\partial t} dx = \int_0^s k_f \frac{\partial^2 T}{\partial x^2} dx \quad (21)$$

The right-hand side integral can be evaluated explicitly. The left-hand side integral is handled by substituting the expression for the total enthalpy, Eq. (20), which yields:

$$\frac{\partial \psi}{\partial t} = k_f \left[\frac{\partial T}{\partial x}(s, t) - \frac{\partial T}{\partial x}(0, t) \right] \quad (22)$$

Further substitution of the assumed temperature distribution, Eq. (19), would obtain:

$$\frac{\partial \psi}{\partial t} = \frac{k_u H_u}{s} [\exp(\varphi s) - 1] \quad (23)$$

The change in total enthalpy during each time interval, Δt , conforming to the numerical solution of the unfrozen region, is given by:

$$\Delta \psi = \int_t^{t+\Delta t} \frac{\partial \psi}{\partial t} dt \quad (24)$$

By assuming a constant velocity of propagation of the freezing front over each time interval, which may still change between time intervals, the change in total enthalpy is obtained:

$$\Delta \psi = \frac{k_u H_u}{s} \left\{ \frac{1}{\varphi s} \exp(\varphi s t) [\exp(\varphi s \Delta t) - 1] - \Delta t \right\} \quad (25)$$

Alternatively, the change in total enthalpy may also be calculated explicitly by substituting the assumed temperature distribution, Eq. (19), into the definition of this property, Eq. (20), to yield:

$$\begin{aligned}
 \Delta \psi &= \psi(t + \Delta t) - \psi(t) \\
 &= \frac{k_u H_u}{s \alpha_f \varphi} \left\{ \frac{1}{\varphi} \exp(\varphi s t) [\exp(\varphi s \Delta t)] - s \Delta t \right\} \quad (26)
 \end{aligned}$$

Equating Eqs. (25) and (26) obtains the expression for the coefficient φ :

$$\varphi = \frac{s}{\alpha_f} \quad (27)$$

and the temperature distribution in the frozen region is given by:

$$T = T_{mf} - \frac{k_u H_u}{C_f s^2} \left\{ 1 - \exp \left[\frac{s}{\alpha_f} (s - x) \right] \right\} \quad (28)$$

which may be rewritten in terms of the thermophysical properties in the frozen region by employing Eq. (3), boundary condition (18b), and by noting that $\alpha = k/C$:

$$T = T_{mf} - \frac{\alpha_f H_f}{s^2} \left\{ 1 - \exp \left[\frac{s}{\alpha_f} (s - x) \right] \right\} \quad (29)$$

where H_f is the cooling rate as viewed from the frozen region.

It is noted that the velocity of propagation of the freezing front may change from one time interval to the next. At a quasi-

steady state, the temperature distribution, given by Eq. (29), conforms precisely to the exact solution obtained by Rabin and Shitzer (1995): hence the motivation for expressing the temperature distribution by Eq. (19). For the general case of a variable velocity of propagation of the freezing front, the solution given by Eq. (29) would be an approximate one. However, due to the application of the enthalpy approach, it may be expected to yield a relatively good estimate for the location of the freezing front.

Results and Discussion

Validation of the combined solution developed here is done by comparing it to an exact solution (Rabin and Shitzer, 1995). This exact solution is actually a particular case of the combined solution for a quasi-steady state. It is, additionally, a particular case in which both the metabolic heating rate and the thermal effects of blood perfusion are constant in time and uniformly distributed in the unfrozen region of the tissue.

For comparison purposes, the problem was evaluated for two limiting cases: one in which there is no blood perfusion and the other in which perfusion is high in peripheral tissues. These two cases are defined by specifying the values of the products of blood perfusion and heat capacity, a quantity that represents the specific heating rate of blood, at 0 and $10 \text{ kW/m}^3 \cdot ^\circ\text{C}$, respectively. The solution to the inverse Stefan problem for these two cases is presented for a constant velocity of propagation of the freezing front of 1.5 mm/min . Thermophysical values are listed in Table 1. This velocity of propagation of the freezing front induces cooling rates of 7°C/min and 8°C/min at the freezing front for the two blood flow rates given above, respectively.

The combined solution is derived for a uniform initial condition. The boundary condition imposed at the outer interface, until the freezing front begins to form, is extracted from the exact solution. The computation was carried out until the temperature at the cryoprobe surface had reached -196°C , which is the lowest temperature limit for cryosurgical applications employing liquid nitrogen as the cryofluid. The numerical solution was performed for 0.1 mm space intervals and 1 s time intervals.

The analytical solution of the frozen region revealed that, throughout the entire process, the velocity of propagation of the freezing front has maintained its initial constant value to within five significant figures. For this situation the exact and the combined solutions coincide, as noted above. It can, therefore, be concluded that in the frozen region the integral solution yields sufficiently accurate predictions.

The unfrozen region, on the other hand, is solved numerically by the proposed combined solution. Thus, comparison of the temperature distributions obtained thereof with those of the exact solution, is required for validation. Figure 2 indicates that the proposed numerical solution produces rather accurate temperature distributions in the unfrozen region. This is further accentuated by noting that the initial temperature in the unfrozen region was uniform and, thus, underwent considerable changes during the process.

The subregion in which the largest deviations between the two solutions may be expected is the phase-change region. During phase transition, the volumetric specific heat changes appreciably from 1.8 and $3.6 \text{ MJ/m}^3 \cdot ^\circ\text{C}$ in the frozen and unfrozen regions, respectively, to about $67 \text{ MJ/m}^3 \cdot ^\circ\text{C}$ at the peak phase transition temperature range (see Fig. 1). Comparison of the exact and combined solutions in this region is shown in Fig. 3. It is seen that very good conformity is obtained. The maximal deviation obtained is smaller than 0.1°C , which represents an error of less than 0.2 percent compared to the maximal temperature change in the unfrozen region throughout the entire process. The “+” signs in Fig. 3 designate all the grid points of the numerical solution. As seen, only four to five grid points are required to reside within the phase-change temperature range

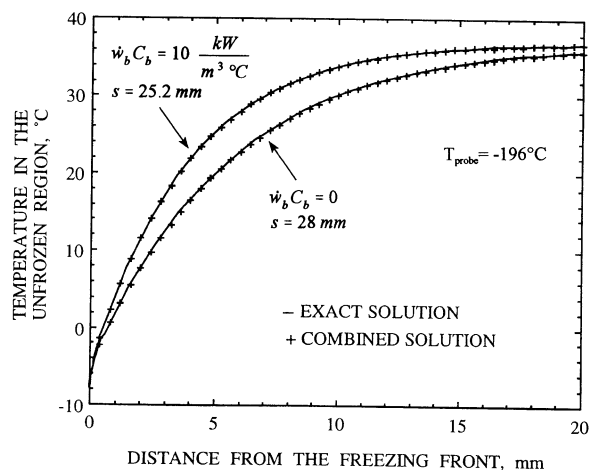


Fig. 2 Comparison of calculated temperature distributions in the unfrozen region with an exact solution (Rabin and Shitzer, 1995) for zero and relatively high blood perfusion rates

for a rather good conformity between the two solutions to be obtained.

Further validation of this solution was done by comparing its predictions to a series of in vivo cryoprocures performed on the skeletal muscle of rabbits' hindlimbs. Details are given by Rabin and Shitzer (1996) and Rabin et al. (1996).

The capabilities of the combined solution in cases of several repeated freezing/thawing cycles, are demonstrated next. Each cycle in this demonstration is composed of four stages:

- Precooling, in which the temperature of the cryoprobe changes linearly until the lower temperature limit of phase change, T_{mf} , is reached and a completely frozen front is initiated.
- Freezing, in which the temperature of the cryoprobe changes according to the forcing function calculated by the combined solution. This stage proceeds until the lowest temperature of the boiling cryofluid is reached at the surface of the cryoprobe (e.g., -196°C for liquid nitrogen).
- Heating, in which the temperature of the cryoprobe changes linearly until it reaches its initial level, and,
- Thawing, in which the temperature of the cryoprobe is maintained at its initial level. Complete thawing is obtained when all regions inside the domain have exceeded the upper temperature limit of phase transition, T_{ml} .

Stages (a), (c), and (d) are analyzed as ordinary Stefan problems. The solution for these stages, in the entire domain, is obtained by a numerical scheme similar to the combined solution in the unfrozen region, Eq. (16). Since in these stages there is no freezing front, β becomes 0 in the modified equation. Moreover, it is assumed that all metabolic and blood perfusion activities do not exist in the frozen regions and thus γ and μ become zero in the frozen region, as well.

Thawing is assumed to occur over the same temperature range as for freezing. It is recognized that these processes are governed by different mechanisms, which may result in different temperature ranges. However, the analysis is capable of handling any specified temperature ranges for each stage in the cryoprocure. This may slightly affect the calculated location of the freezing front. It will, however, have essentially no effect on the duration of the freezing/thawing cycle due to the use of an effective specific heat function over the entire temperature range, as discussed above.

Computational capabilities of the solution were demonstrated for two cases of zero and extremely high blood perfusions, represented by 0 and $25 \text{ kW/m}^3 \cdot ^\circ\text{C}$, respectively. It is assumed, for demonstration purposes, that complete destruction of blood vessels occurs by the freezing process. Thus, the solution in

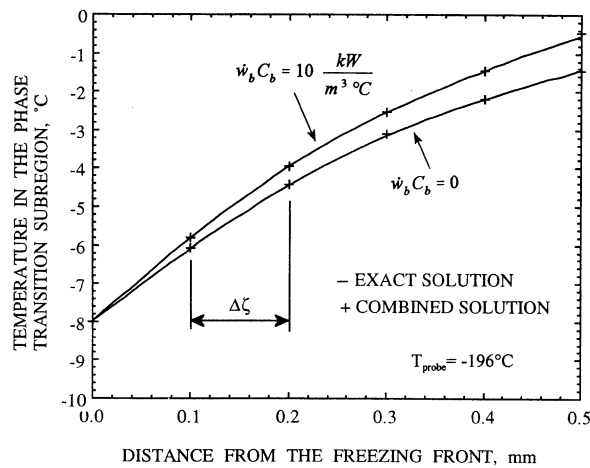


Fig. 3 Comparison of calculated temperature distributions, in the phase change region, with an exact solution (Rabin and Shitzer, 1995), at the end of the cooling stage (when the cryoprobe reaches -196°C) for zero and high blood perfusion rates

the unfrozen region of the second case does not include blood perfusion in the thawed region. This assumption accentuates the flexibility of the numerical solution in the unfrozen region. The following parameters were used in this demonstration: cryoprobe cooling rate of $40^\circ\text{C}/\text{min}$ in stage (a); cooling rates of $5^\circ\text{C}/\text{min}$ and $10^\circ\text{C}/\text{min}$ at the freezing front in stage (b), which relate to maximal cell destruction (Orpwood, 1981); cryoprobe heating rate of $50^\circ\text{C}/\text{min}$ in stage (c), which is a reasonable rate for cryoprotocols; and initial temperature of 37°C in stage (d). Stage (b) was terminated when the boiling temperature of liquid nitrogen, -196°C , had been reached.

Figures 4–6 present results of the first five successive freezing/thawing cycles. It can be seen in Fig. 4 that there is only a relatively small difference, in the calculated temperature forcing function at the cryoprobe–tissue interface of stage (b), between the first and the fifth cycles. Moreover, there are only minor differences between the two cases considered of zero and extremely high blood perfusion. The total durations of the cooling period of stages (a) and (b) in the fifth cycle are shorter by 5 and 9 percent than the first cycle, for the cases of zero and extremely high blood perfusion in peripheral tissues, respectively. In general, there is an apparent similarity between the temperature forcing functions for the cases of freezing rates of $5^\circ\text{C}/\text{min}$ and $10^\circ\text{C}/\text{min}$. However, the differences between the

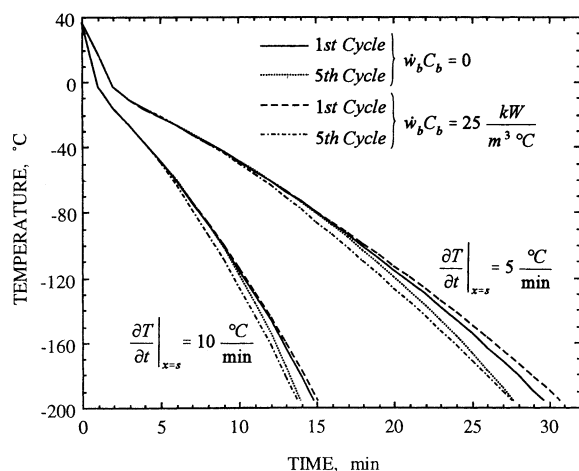


Fig. 4 Calculated temperature forcing functions at the cryoprobe–tissue interface during the freezing process, for the first and the fifth freezing/thawing cycles for different blood perfusion rates

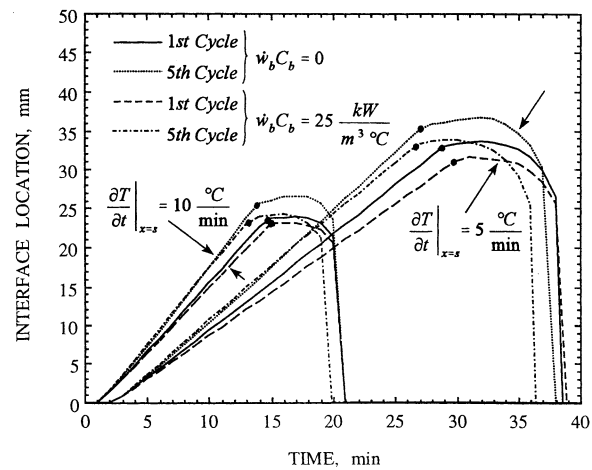


Fig. 5 Freezing front location, for the first and the fifth repeated freezing/thawing cycles for different blood perfusion rates and cooling rates. The “●” signs indicate the end of the freezing stage (b) and the initiation of the heating stage (c).

temperature forcing functions within each freezing rate decrease as these cooling rates increase.

It can be seen in Fig. 5 that the freezing front velocity is almost linear in time during the freezing stage, in both the first and the fifth cycles. The freezing front location seems to be weakly dependent on blood perfusion in the first cycle. However, the freezing front penetrates deeper in the case of no blood perfusion, during the beginning of the thawing stage, due to thermal inertia. The maximal depth of freezing in the fifth cycle is about 7 percent larger than in the first cycle, in all the cases considered.

Figure 6 presents the calculated durations of the freezing and thawing stages in each cycle for all the cases considered. The freezing stage in the first cycle is about 10 percent longer than in the fifth one for all cases. This is because the microvasculature is

| $\frac{\partial T}{\partial t} \Big _{x=s} = 5 \frac{^\circ\text{C}}{\text{min}}$ | | $10 \frac{^\circ\text{C}}{\text{min}}$ | |
|---|---|---|---|
| ■ | □ | ■ | □ |
| ▣ | ▣ | ▣ | ▣ |
| ▤ | ▤ | ▤ | ▤ |
| ▥ | ▥ | ▥ | ▥ |
| Freezing | | Freezing | |
| Thawing | | Thawing | |
| $\dot{w}_b C_b = 0$ | | $\dot{w}_b C_b = 25 \frac{kW}{m^3 \text{ } ^\circ C}$ | |

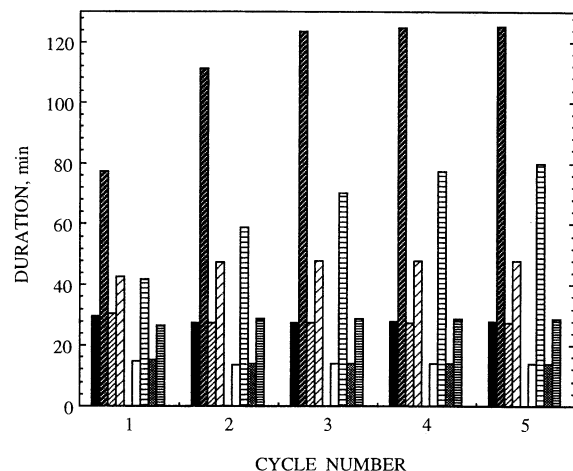


Fig. 6 Cycle duration and thawing period of the first five successive freezing/thawing cycles, in cases of no blood perfusion and a relatively high blood perfusion in peripheral tissues

assumed to be destroyed by freezing in the first cycle (see above) and since a lower average initial temperature is obtained in each successive cycle. Actually, the freezing durations in the third and fifth cycles are almost identical. As can be expected, the thawing duration is strongly dominated by blood perfusion. In the case of extremely high blood perfusion, the thawing durations of the first cycle are about 10 percent shorter than in the fifth one. Another dominant factor is the cooling rate. It is seen that the thawing durations in the case of zero blood perfusion are about 38 and 45 percent shorter in the first cycle with respect to the fifth one, for the cases of freezing rates of 5°C/min and 10°C/min, respectively. Similar values are obtained for the freezing stage.

It is noted in Fig. 6 that cycle durations are rather long and, in certain cases, may well exceed one hour. From a clinical view point this may be undesirable or even unacceptable. However, these rather long durations of application are chiefly determined by the cooling rate required at the freezing front; the lower the cooling rate, the longer the duration of the freezing/thawing cycle. The desired cooling rate is determined by biological and physical considerations. Thus, cycle durations will depend on this factor, the depth of freezing required, and, to a somewhat lesser extent, on blood perfusion in the first cycle of freezing/thawing.

From Figs. 4–6 it can be deduced that there are only minor differences in the shape of the temperature forcing function and in the freezing front location, as the number of freeze/thaw cycles increases. The largest differences are observed between the first and the second cycles in each case, as is to be expected. The thermal effect of blood perfusion does not appreciably affect the forcing function, nor does it affect the freezing front location. However, it has a major influence on cycle duration, especially during the thawing stage. The parametric study was repeated for the case of a physiologically unrealistic specific heat source of blood of 100 kW/m³-°C, which is used to test the nature of the mathematical solution. In this case the extent of penetration of the freezing front is only about 50 percent as compared to the case of zero blood perfusion.

An additional third case was also investigated, with an extremely high blood perfusion as in the second case, but under the assumption of full recovery of the vascular system, i.e., the blood perfusion returns to its pre-treatment level in the thawed region. Results of this third case were found to be bound by the results of these two cases.

Conclusions

This paper presents a combined integral-numerical solution to the one-dimensional inverse Stefan problem in a semi-infinite medium. The frozen region was solved by the integral technique applied to the heat balance equation. A modified Crank–Nicholson numerical scheme was used to solve the temperature distribution in the unfrozen region. This scheme, which was based on the enthalpy method, was adapted to include the thermal effects of metabolism and blood perfusion.

Very good conformity was obtained between the results of the present analysis and a previously published exact solution of the problem. The proposed solution is unique in its ability to consider the thermal effects of temperature-dependent metabolism and blood perfusion. Also, this solution is applicable to successive freezing/thawing cycles in cryosurgical procedures derived from its ability to accommodate any arbitrary initial condition of the problem.

The temperature forcing function at the cryoprobe–tissue interface, the freezing front location, and the cycling durations were calculated, using the combined solution in the freezing stage, and using a complete numerical solution during the pre-cooling and thawing periods. It was found that the thermal effect of blood perfusion does not appreciably affect the shape of

the temperature forcing function, or the freezing front location. However, it was found that metabolism and blood perfusion have major influences on the cycle duration, and especially during the thawing stage. The cooling rate imposed at the freezing front also has a dominant effect on cycle durations.

Acknowledgments

This research was supported, in part, by the James H. Belfer Chair in Mechanical Engineering and by the Vice President for Research Fund for the promotion of research at the Technion.

References

- Akhtar, T., Pegg, D. E., and Foreman, J., 1979, "The Effect of Cooling and Warming Rates on the Survival of Cryopreserved L-Cells," *Cryobiology*, Vol. 16, pp. 424–429.
- Altman, P. L., and Dittmer, D. S., 1971, *Respiration and Circulation*, Federation of American Societies for Experimental Biology (Data Handbook), Bethesda, MD.
- Augustynowicz, S. D., and Gage, A. A., 1985, "Temperature and Cooling Rate Variations During Cryosurgical Probe Testing," *International Journal of Refrigeration*, Vol. 8, pp. 198–208.
- Budman, H. M., Shitzer, A., and Dayan, J., 1995, "Analysis of the Inverse-Stefan Problem of Freezing and Thawing of a Binary Solution During Cryosurgical Processes," *ASME JOURNAL OF BIOMECHANICAL ENGINEERING*, Vol. 117, pp. 193–202.
- Carnahan, B., Luther, H. A., and Wilkes, J. O., 1969, *Applied Numerical Methods*, Wiley, New York.
- Carlsaw, H., and Jaeger, J., 1959, *Conduction of Heat in Solids*, 2nd ed., Oxford University Press, London, Chap. 11, pp. 282–286.
- Comini, G., and del Giudice, S., 1976, "Thermal Aspects of Cryosurgery," *ASME Journal of Heat Transfer*, Vol. 98, pp. 543–549.
- Eberhart, R. C., 1985, "Thermal Models of Single Organs," in: *Heat Transfer in Medicine and Biology: Analysis and Applications*, A. Shitzer and R. C. Eberhart, eds., Plenum Press, New York, p. 275.
- Fahy, G. M., 1981, "Analysis of Solution Effect Injury: Cooling Rate Dependence of the Functional and Morphological Sequellae of Freezing in Rabbit Renal Cortex Protected With Dimethyl Sulfoxide," *Cryobiology*, Vol. 18, pp. 550–570.
- Farrant, J., 1971, "Cryobiology: The Basis of Cryosurgery," in: *Cryogenics in Surgery*, H. von Leden and W. G. Cahan, eds., Lewis, London, pp. 15–42.
- Gage, A. A., Guest, K., Montes, M., Caruna, J. A., and Whalen, D. A., Jr., 1985, "Effect of Varying Freezing and Thawing Rates in Experimental Cryosurgery," *Cryobiology*, Vol. 22, pp. 175–182.
- Goodman, T. R., 1958, "The Heat Balance Integral and Its Application to Problems Involving a Change of Phase," *Transactions of the ASME*, Vol. 80, pp. 335–342.
- Mazur P., 1963, "Kinetics of Water Loss From Cells of Subzero Temperatures and the Likelihood of Intracellular Freezing," *The Journal of General Physiology*, Vol. 47, pp. 347–369.
- Miller, R. H., and Mazur, P., 1976, "Survival of Frozen-Thawed Human Red Cells as a Function of Cooling and Warming Velocities," *Cryobiology*, Vol. 13, pp. 404–424.
- Orpwood, R. D., 1981, "Biophysical and Engineering Aspects of Cryosurgery," *Physics in Medicine and Biology*, Vol. 26, pp. 555–575.
- Pennes, H. H., 1948, "Analysis of Tissue and Arterial Blood Temperature in the Resting Human Forearm," *Journal of Applied Physiology*, Vol. 1, pp. 93–122.
- Rabin, Y., and Shitzer, A., 1995, "Exact Solution to the Inverse Stefan-Problem in Non-ideal Biological Tissues," *ASME Journal of Heat Transfer*, Vol. 117, pp. 425–431.
- Rabin, Y., and Shitzer, A., 1996, "A New Cryosurgical Device for Controlled Freezing: Part I: Setup and Validation Tests," *Cryobiology*, Vol. 33, pp. 82–92.
- Rabin, Y., Coleman, R., Mordohovich, D., Ber, R., and Shitzer, A., 1996, "A New Cryosurgical Device for Controlled Freezing: Part II: In Vivo Experiments on Skeletal Muscle of Rabbit Hindlimbs," *Cryobiology*, Vol. 33, pp. 93–106.
- Rand, R. W., Rand, R. P., Eggerding, F. A., Field, M., Denbesten, L., King, W., and Camici, S., 1985, "Cryolumpectomy for Breast Cancer: An Experimental Study," *Cryobiology*, Vol. 22, pp. 307–318.
- Rubinsky, B., and Onik, G., 1991, "Cryosurgery: Advances in the Application of Low Temperatures to Medicine," *International Journal of Refrigeration*, Vol. 14, pp. 190–199.
- Rubinsky, B., and Shitzer, A., 1976, "Analysis of a Stefan-like Problem in a Biological Tissue Around a Cryosurgical Probe," *ASME Journal of Heat Transfer*, Vol. 98, pp. 514–519.
- Shamsundar, N., and Sparrow, E. M., 1975, "Analysis of Multidimensional Conduction Problem Via the Enthalpy Model," *ASME Journal of Heat Transfer*, Vol. 97, pp. 333–340.
- Stefan, J., 1891, "Ueber die Theorie der Eissbildung, Insbesondere Ueber die Eissbildung in Polymeren," *Annals Physical Chemistry*, Vol. 42, pp. 269–286.
- Voller, V. R., 1986, "A Heat Balance Integral Based on the Enthalpy Formulation," *International Journal of Heat and Mass Transfer*, Vol. 30, pp. 604–606.
- Wessling, F. C., and Blackshear, P. L., 1973, "The Thermal Properties of Human Blood During the Freezing Process," *ASME Journal of Heat Transfer*, Vol. 95, pp. 246–249.